Influence of photoperiod duration and light-dark transitions on entrainment of Per1 and Per2 gene and protein expression in subdivisions of the mouse suprachiasmatic nucleus

Sosniyenko, Serhiy; Hut, Roelof A.; Daan, Serge; Sumova, Alena

Published in:
European Journal of Neuroscience

DOI:
10.1111/j.1460-9568.2009.06945.x

Publication date:
2009

EJN fens European Journal of Neuroscience

European Journal of Neuroscience, Vol. 30, pp. 1802–1814, 2009 doi:10.1111/j.1460-9568.2009.06945.x

NEUROSYSTEMS

Influence of photoperiod duration and light–dark transitions on entrainment of *Per1* and *Per2* gene and protein expression in subdivisions of the mouse suprachiasmatic nucleus

Serhiy Sosniyenko,[1] Roelof A. Hut,[2] Serge Daan[2] and Alena Sumová[1]
[1]Department of Neurohumoral Regulations, Institute of Physiology, v.v.i., Academy of Sciences of the Czech Republic, Czech Republic
[2]Department of Chronobiology, University of Groningen, Haren, the Netherlands

Keywords: clock gene, clock protein, photoperiodic synchronization, SCN

Abstract

The circadian clock located within the suprachiasmatic nuclei (SCN) of the hypothalamus responds to changes in the duration of day length, i.e. photoperiod. Recently, changes in phase relationships among the SCN cell subpopulations, especially between the rostral and caudal region, were implicated in the SCN photoperiodic modulation. To date, the effect of abrupt, rectangular, light-to-dark transitions have been studied while in nature organisms experience gradual dawn and twilight transitions. The aim of this study was to compare the effect of a long (18 h of light) and a short (6 h of light) photoperiod with twilight relative to that with rectangular light-to-dark transition on the daily profiles of *Per1* and *Per2* mRNA (*in situ* hybridization) and PER1 and PER2 protein (immunohistochemistry) levels within the rostral, middle and caudal regions of the mouse SCN. Under the short but not under the long photoperiod, *Per1*, *Per2* and PER1, PER2 profiles were significantly phase-advanced under the twilight relative to rectangular light-to-dark transition in all SCN regions examined. Under the photoperiods with rectangular light-to-dark transition, *Per1* and *Per2* mRNA profiles in the caudal SCN were phase-advanced as compared with those in the rostral SCN. The phase differences between the SCN regions were reduced under the long, or completely abolished under the short, photoperiods with twilight. The data indicate that the twilight photoperiod provides stronger synchronization among the individual SCN cell subpopulations than the rectangular one, and the effect is more pronounced under the short than under the long photoperiod.

Introduction

Mammals exhibit an array of daily behavioral, physiological, hormonal, biochemical and molecular rhythms. Under natural conditions, the rhythms are entrained to the 24-h day by the light–dark (LD) cycle, mostly by the light period of the day (Pittendrigh, 1981). In temperate latitudes, the day length, i.e. photoperiod, changes during the year. In nocturnal rodents, duration of the locomotor activity and nocturnal melatonin signal are photoperiod-dependent, being shorter on long summer than on short winter days (Illnerová & Vaněček, 1980; Illnerová, 1988; Elliott & Tamarkin, 1994). The locomotor activity rhythm, the rhythm in melatonin production and other circadian rhythms are controlled by a central pacemaker located in the suprachiasmatic nucleus (SCN) of the hypothalamus (Klein & Moore, 1979; LeSauter *et al.*, 1996). The SCN is also affected by the photoperiod (Sumová *et al.*, 1995). Its rhythmicity is generated by the molecular clockwork (for review, see Takahashi *et al.*, 2008). Several mammalian genes, namely two Period genes (*Per1* and *Per2*), two Cryptochrome genes (*Cry1* and *Cry2*), *Clock*, *Bmal1*, *Rev-erbα, Rora* and casein kinase 1 epsilon (*CK1ε*), are thought to be mainly involved in the clockwork mechanism by forming interacting transcriptional–translational feedback loops. Most of these genes are expressed rhythmically; the expression of *Bmal1* is anti-phase to that of the *Per* and *Cry* genes. *Per* transcription is activated by the CLOCK-BMAL1 protein complex through its binding to E-box sequences located in the *Per* promoter region. The entire mechanism is not yet fully understood.

The functional state of the SCN itself is affected by the photoperiod and may thus serve as a basis not only for the daily clock, but also for the seasonal clock. In rodents, the interval of elevated *Per1* and *Per2* expression in the SCN is longer under a long photoperiod than under a short one (Hastings, 2001; Steinlechner *et al.*, 2002; Sumová *et al.*, 2002, 2003). Recent data showed that expression of some of the clock genes under various photoperiods is not necessarily synchronized throughout the entire SCN. Marked regional differences in gene expression rhythms along the rostro–caudal axis of the hamster SCN were reported. *Per2* expression was photoperiod-dependent in both the

Correspondence: Dr A. Sumová, as above.
E-mail: sumova@biomed.cas.cz

Received 25 February 2009, revised 11 August 2009, accepted 18 August 2009

rostral and caudal SCN; under a short photoperiod, the maximal expression occurred in synchrony in both parts, but under a long photoperiod the peak of expression in the caudal SCN preceded that in the rostral SCN (Hazlerigg *et al.*, 2005; Johnston *et al.*, 2005; Yan & Silver, 2008).

The vast majority of laboratory studies have used animals maintained under a LD cycle with abrupt, rectangular (RA), transitions between light and darkness. However, in nature, animals experience gradual LD transitions at dusk and dawn; the dynamics and duration of these transitions depend on season and latitude (Daan & Aschoff, 1975; Boulos *et al.*, 1996b; Boulos & Macchi, 2005). The spectral composition of artificial light cycles also differs from that of natural light, which varies during the twilight hours (McFarland & Munz, 1975; Hut *et al.*, 2000). Light-sensitive SCN neurons exhibit sustained responses to light stimuli of long duration and response to increasing and decreasing light intensity (Meijer *et al.*, 1986). Under natural conditions, the circadian system may thus continuously monitor changes in environmental illumination and utilize this information for entrainment (Usui, 2000). The inclusion of twilight LD transition (TW) in the regimens affected several circadian locomotor parameters in a season- and latitude-dependent manner. In Syrian hamsters, the timing of activity onset followed dusk in the presence of TW, but was more closely related to dawn in its absence. The offsets and midpoint of activity occurred earlier under a TW than under an RA regimen, with the difference most pronounced being observed under a short photoperiod. The presence of TW also resulted in lower day-to-day variability in activity onset times (Boulos & Macchi, 2005). In addition to the locomotor activity, also the pineal rhythm in arylalkyl-N-acetyltransferase activity was studied under natural photoperiods (Illnerová & Vaněček, 1980). So far, the effect of TW on the molecular clockwork in the mammalian SCN has been only marginally studied. In our previous work, PER1 protein profiles in the middle part of the SCN of rats maintained under natural photoperiods in summer and winter resembled those of rats maintained under the corresponding artificial photoperiods (Sumová *et al.*, 2002).

The aim of the present study was to determine in detail whether and how photoperiods with artificial TW affect expression of the clock genes, namely of *Per1* and *Per2*, and their products PER1 and PER2, in the mouse SCN and to compare the effect of the TW photoperiod with that of the RA photoperiod. Mice were entrained to a long photoperiod with 18 h of light and 6 h of darkness, or a short photoperiod with 6 h of light and 18 h of darkness under abrupt RA or gradual TW LD transition. Thereafter, they were released into darkness, and daily profiles of *Per1* and *Per2* expression and PER1 and PER2 levels were measured within the rostral (R), middle (M) and caudal (C) parts of the SCN.

Materials and methods

Animals

Two-month-old adult male C57Bl6/J mice (Velaz s.r.o., Czech Republic and Harlan, Horst, The Netherlands) were housed at a temperature of 23 ± 2°C with free access to food and water. For 4 weeks prior to the experiments, the animals were maintained under a long and short photoperiod with two different models of LD transition, namely the abrupt RA and gradual TW. For RA photoperiods, light was provided by overhead 40-W fluorescent tubes, and illumination during the light phase was between 50 and 200 lx, depending on cage position in the animal room. There was complete darkness during the dark period. Lights were on from 03.00 to 21.00 h for a long (LD18 : 6) photoperiod, and from 09.00 to 15.00 h for a short (LD6 : 18) photoperiod. For TW photoperiods, the light level during the dark phase was lower than 0.001 lx and the maximum light level during the light phase was 100 lx at the level of the cage. The gradual transition between darkness and light (and vice versa) took 1.5 h. It was controlled by the ACIS system (Spoelstra & Daan, 2008), which diminished light intensity without causing spectral changes by means of a computer-controlled shutter system.

Light intensity during twilight expressed logarithmically changed linear over time with a step size of 0.01 lx per 2 min. For the long photoperiod, the gradual decline of light intensity from 100 lx started at 20.15 h, and reached 0.01 lx at 21.45 h. The gradual increase in light intensity started from 0.01 lx at 02.15 h and reached 100 lx at 03.45 h. For the short photoperiod, the light intensity decline from 100 to 0.01 lx occurred between 14.15 and 15.45 h, and the light intensity rise from 0.01 to 100 lx occurred between 08.15 and 09.45 h. The log (intensity) mid-point of the TW increasing and decreasing slopes (at 1 lx) coincided with lights on and lights off in the RA light profiles for both photoperiods (Fig. 1A).

On the day of experiments, animals entrained to the short and long photoperiods with either RA or TW conditions were released into constant darkness, i.e. the morning light was not turned on. Every 2 h throughout the whole circadian cycle in complete darkness, four animals were sampled for *Per1* and *Per2* mRNA and three animals for PER1 and PER2 protein determination. For each photoperiod, the sampling was completed within 1 day. For experiments with RA transition, mice were maintained in animal facilities of the Institute of Physiology, v.v.i., Academy of Sciences of the Czech Republic, Prague. For experiments with TW transition, mice were kept in animal facilities of the University of Groningen, Haren, The Netherlands. The experiments were conducted under license no. A5228-01 with the US National Institutes of Health and in accordance with Animal Protection Law of the Czech Republic (license no. 42084/2003-1020) and license no. DEC #4660A of the Animal Experimentation committee of the University of Groningen.

In situ *hybridization*

For determination of *Per1* and *Per2* mRNA levels, mice were killed by decapitation immediately after cervical dislocation, brains were removed, immediately frozen on dry ice and stored at −80°C. Each brain was sectioned into five series of 12-μm coronal slices in alternating order throughout the entire rostro–caudal extent of the SCN and processed for *in situ* hybridization.

The cDNA fragments of rat rPer1 (980 bp; corresponds to nucleotides 581–1561 of the sequence in GenBank with accession no. AB002108) and rat rPer2 (1512 bp; corresponds to nucleotides 369–1881 of the sequence in Genbank with accession no. NM031678) were used as templates for *in vitro* transcription of complementary RNA probes. The r*Per1* and r*Per2* fragment-containing vectors were generously donated by Professor H. Okamura (Kobe University School of Medicine, Japan).

The probes were labeled using α[^{35}S]thio-UTP (MP Biomedicals, Irvine, CA, USA), and the *in situ* hybridization was performed as described previously (Shearman *et al.*, 2000; Sládek *et al.*, 2004; Kováčiková *et al.*, 2006). Briefly, sections were hybridized for 20 h at 60°C (Per1) or 61°C (Per2). Following a post-hybridization wash, the sections were dehydrated in ethanol and dried. Finally, the slides were exposed to the BioMax MR film (Kodak) for 10 days and developed using the developer ADEFO-MIX-S and fixer ADEFO-FIX (ADEFO-CHEMIE Gmbh, Dietzenbach, Germany) in film processor Optimax (PROTEC GmBH, Oberstenfeld, Germany). As a

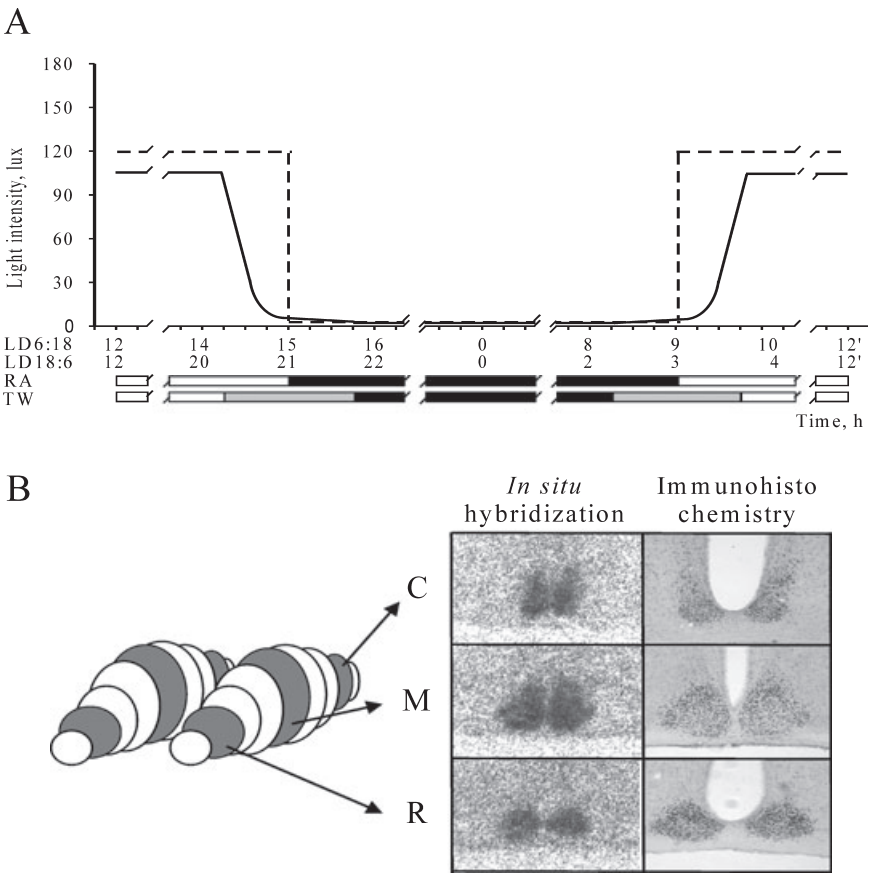

FIG. 1. Schematic cartoon of (A) experimental design of the light intensity changes during the rectangular (RA) and twilight (TW) photoperiod. Black bars depict intervals of the previous complete darkness, shaded bars depicts intervals of the TW. The *x*-axis is expressed in real time under the short (LD6 : 18 – upper line) and under the long (LD18 : 6 – lower line) photoperiod. (B) The SCN with marked rostral (R), middle (M) and caudal (C) sections (left), and representative *in situ* hybridization signals of *Per1* mRNA and of the immunohistochemistry staining of PER1 protein on sections from the corresponding parts of the SCN (right).

control, *in situ* hybridization was performed in parallel with sense probes on sections containing the SCN. For photoperiods with RA and TW transitions, the whole daily profiles of mRNA levels following the LD18 : 6 and LD6 : 18 were determined using the same labeled probe and processed simultaneously under identical conditions.

Autoradiographs of sections were analysed using an image analysis system (Image Pro, Olympus, New Hyde Park, NY, USA) to detect the relative optical density (OD) of the specific hybridization signal. In each animal, the mRNA was quantified bilaterally, at a representative R-, M- and C-SCN section (Fig. 1B). To define the position of the R-, M- and C-SCN on the film autoradiograph, the slides were counter-stained with Cresyl violet. The determination of the rostro–caudal position was based on typical shape of the nucleus at the coronal section (see Fig. 1B), as well as on distance from the utmost rostral section of the SCN; a section was considered to be rostral, middle and caudal when positioned within the 50–150-μm-, 250–350-μm- and 450–550-μm-thick compartment of the SCN, respectively. Each measurement was corrected for a non-specific background by subtracting OD values from the neighboring area in the hypothalamus that was free of specific signal. The background signal of the area, serving as an internal standard, was consistently low and did not exhibit marked changes with the time of day. In no case did *in situ* hybridization yield any specific signal using a sense probe. The OD for each animal was calculated as the mean of the values for the left and right SCN.

Immunohistochemistry

For determination of PER1 and PER2 protein levels, mice were deeply anesthetized with thiobarbital sodium (50 mg per kg, i.p.; Valeant Czech Pharma s.r.o., Praha, Czech Republic) and perfused through the ascending aorta with heparinized saline followed by phosphate-buffered saline (PBS; 0.01 M sodium phosphate, 0.15 M NaCl, pH 7.2) and then freshly prepared 4% paraformaldehyde in PBS. Brains were removed, post-fixed for 12 h at 4°C, and cryoprotected in 20% sucrose in PBS overnight at 4°C, frozen on dry ice and stored at −80°C. Each brain was sectioned into five series of 30-μm-thick coronal slices in alternating order throughout the whole rostro–caudal extent of the SCN and processed by free-floating immunohistochemistry using the standard avidin–biotin method with diaminobenzidine as the chromogen (Vector Laboratories, Peterborough, UK; Sumova *et al.*, 2002). The polyclonal primary PER1 antiserum was synthesized at the Massachusetts General Hospital Biopolymer Core Facility. It was raised in rabbits against amino acids 6–21 of the peptide sequence of mPER1 and characterized elsewhere (Sun *et al.*, 1997; Hastings *et al.*, 1999). The polyclonal primary PER2 antiserum was purchased from ADI (Greenwich, CT, USA). Specificity of the tissue staining was checked with and without blocking peptide (ADI, PER21-P; data not shown). All sections were developed in diaminobenzidine for exactly the same time to achieve the same intensity of the background staining. For photoperiods with RA and TW, the whole daily profiles of protein levels following the long and short photoperiod were

determined within one assay under identical conditions. Labeled cell nuclei were counted in sections representing the R-, M- and C-SCN (Fig. 1B) by two independent observers using an image analysis system (ImagePro, Olympus, New Hyde Park, NY, USA). The intensity of background staining was set at the nearest area surrounding the SCN, and every cell, with an intensity level above the background, was counted. For the C-SCN, some sections were damaged and, therefore, were excluded from counting. This decreased the number of samples at 12.00, 02.00 and 04.00 h under the short photoperiods from three to only two.

Statistical analysis

To ascertain whether daily profiles of *Per1* and *Per2* mRNA and PER1 and PER2 protein levels in the R-, M- and C-SCN under the long photoperiod differed from those under the short photoperiod, the profiles under these photoperiods both with RA and TW were compared by two-way analysis of variance (ANOVA, BMDP Statistical Software, University of California, Berkley, CA, USA). The two-way ANOVA was also used to reveal whether the profiles under the TW photoperiods differed from those under the RA photoperiods. Moreover, the two-way ANOVA was used to reveal whether the profiles in the R-, M- and C-SCN differ. In case of significant differences between the profiles and significant interaction effects as well as in case of significant differences between the profiles and non-significant interaction effect, the *post hoc* analysis by the Student's-Newman-Keuls multiple range test was performed with $P < 0.05$ being required for significance. The analysis was also used when a significant interaction effect suggested that the expression profiles might differ, even though the ANOVA did not reveal a significant difference.

The cross-correlation analysis was used to test phase differences between profiles when *post hoc* analysis revealed that the times of the rise and/or decline of gene expression and protein levels differed between the profiles. To asses non-parallel shifts of the rise and decline, the rising and declining parts of the profiles were analysed separately.

Results

Comparison of daily profiles of Per1 *mRNA and PER1 protein levels in mice entrained to the long and short photoperiod with RA and TW within the R-, M- and C- part of the SCN*

Per1 *mRNA*

Comparison of the *Per1* mRNA profiles between the long and short photoperiod revealed that the profiles under the long photoperiod differed significantly from those under the short photoperiod within the R-, M- and C-SCN, whether the LD transition was RA or TW (Table 1). Comparison of the *Per1* mRNA profiles between the RA and TW photoperiods revealed that these profiles were significantly modulated by the type of LD transition (Table 1). Subsequent analysis revealed the following differences between the photoperiods with RA and TW.

Under the short TW photoperiod, *Per1* mRNA levels within the R-SCN (Fig. 2A) first declined at 14.00 h (vs. 12.00 h, $P < 0.05$) and the decline continued until 16.00 h (vs. 14.00 h, $P < 0.05$). Under the short RA photoperiod, the first decline occurred at 16.00 h and continued until 18.00 h (vs. 14.00 and 16.00 h, respectively, $P < 0.01$). The first significant rise occurred at 04.00 h in TW as well as in RA (vs. 02.00 h, $P < 0.05$ under TW; vs. 22.00 h, $P < 0.05$ in RA), but under RA the rise continued further until 12.00 h. Cross-correlation analysis revealed a significant 2-h phase-advance in the decline of *Per1* mRNA levels under TW as compared with RA ($R = 0.986$, $P < 0.001$). In the M-SCN (Fig. 2B), the decline in *Per1* mRNA levels occurred at about the same time, i.e. at 16.00 h (vs. 14.00 h, $P < 0.01$) under RA and TW. However, the first significant rise occurred earlier under TW (at 04.00 vs. 02.00 h, $P < 0.01$) than under RA (at 06.00 vs. 04.00 h, $P < 0.01$). The cross-correlation test revealed a significant 2-h phase-advance in the rise of *Per1* mRNA levels under TW as compared with RA ($R = 0.989$, $P < 0.001$). In the C-SCN (Fig. 2C), *Per1* mRNA levels declined earlier under TW than RA; the decline occurred at 14.00 h (vs. 12.00 h, $P < 0.05$) in TW, but only at 16.00 h (vs. 14.00 h, $P < 0.01$) in RA. The rise was significant at 04.00 h (vs. 02.00 h, $P < 0.05$) under TW, but only at 06.00 h (vs. 04.00 h, $P < 0.01$) under RA. Cross-correlation analysis revealed a significant 2-h phase-advance in the rise of *Per1* mRNA levels under TW as compared with RA ($R = 0.973$, $P = 0.014$) as well as of the decline ($R = 0.948$, $P = 0.004$).

Under the long photoperiod, *Per1* mRNA levels in the R-SCN (Fig. 2D) began to decline earlier under TW (at 20.00 vs. 18.00 h, $P < 0.01$) than under RA (at 22.00 vs. 20.00 h, $P < 0.01$), but the minimum levels were achieved at the same time under RA and TW, i.e. at 22.00 h. The first significant rise in *Per1* mRNA levels occurred at 06.00 h (vs. 00.00 h, $P < 0.05$) under TW, but only at 14.00 h (vs. 12.00 h, $P < 0.05$) under RA. However, the cross-correlation analysis did not reveal a significant phase-advance, probably because of a non-parallel run of both profiles during the daytime hours: while under TW the profile exhibited a gradual rise; under RA intermediate levels were detected. In the M-SCN (Fig. 2E), the decline in *Per1* mRNA levels occurred at the same time under RA and TW, i.e. at 20.00 h (vs. 18.00 h, $P < 0.01$), and the rise was first significant at 06.00 h (vs. 22.00 h, $P < 0.05$) in RA and at 08.00 h (vs. 00.00 h, $P < 0.05$) in TW. The cross-correlation analysis revealed a significant phase-advance in the *Per1* mRNA rise under RA as compared with that under TW ($R = 0.961$, $P = 0.009$). In the C-SCN (Fig. 2F), the *Per1* mRNA levels declined at the same time under RA and TW, i.e. at 20.00 h (vs. 18.00 h, $P < 0.01$); the rise occurred significantly earlier under RA (at 04.00 vs. 22.00 h, $P < 0.05$) than under TW (06.00 vs. 04.00 h, $P < 0.01$). The cross-correlation analysis revealed a significant phase-advance in the *Per1* mRNA rise under the RA as compared with TW ($R = 0.974$, $P = 0.005$).

Comparison of *Per1* mRNA profiles among the R-, M- and C-SCN by the two-way ANOVA under the short photoperiod (Fig. 3A and C) revealed a significant difference between the individual regions of the SCN under RA, but not under TW (Table 1). The *post hoc* analysis revealed that under the short RA photoperiod, the *Per1* mRNA levels were significantly higher in the R-SCN than in M- and C-SCN at 14.00 h ($P < 0.01$) and 16.00 h ($P < 0.01$). The levels were also significantly higher in the R-SCN than in M-SCN at 04.00 h ($P < 0.05$) and 06.00 h ($P < 0.05$), and in the C-SCN than in M-SCN at 06.00 h ($P < 0.05$). The cross-correlation analysis did not reveal any significant phase-shift among the profiles in the R-, M- and C-SCN under the short RA. However, when the phase-shift in the decline was tested separately, the cross-correlation analysis revealed a 2-h phase-delay of the decline in the R-SCN as compared with the C- and M-SCN ($R = 0.978$ and 0.984, respectively; both $P < 0.001$). Under the long photoperiod (Fig. 3B and D), the two-way ANOVA revealed a significant difference among the R-, M- and C-SCN under RA, but not under TW, conditions. However, a significant interaction effect in TW still suggested differences between the profiles of the individual SCN regions (Table 1). In RA, the profiles between R- and C-SCN differed at 12.00, 18.00, 20.00, 00.00, 06.00, 08.00, 10.00 and

TABLE 1A. Short vs. long photo periods (two-way ANOVA comparing *Per1* and *Per2* mRNA and PER1 and PER2 protein levels)

	Per1						*Per2*					
	Photoperiod		Time		Interaction		Photoperiod		Time		Interaction	
	F_1-value	*P*-value	F_{12}-value	*P*-value	F_{12}-value	*P*-value	F_1-value	*P*-value	F_{12}-value	*P*-value	F_{12}-value	*P*-value
mRNA												
RA R	0.05	0.82	26.36	< 0.001	21.92	< 0.001	22.33	< 0.001	46.32	< 0.001	20.13	< 0.001
RA M	10.22	0.002	57.58	< 0.001	10.99	< 0.001	31.08	< 0.001	79.09	< 0.001	25.76	< 0.001
RA C	15.70	< 0.001	72.07	< 0.001	7.66	< 0.001	17.61	< 0.001	85.54	< 0.001	13.21	< 0.001
TW R	21.09	< 0.001	24.80	< 0.001	22.00	< 0.001	0.37	0.55	78.16	< 0.001	37.62	< 0.001
TW M	25.95	< 0.001	40.48	< 0.001	17.23	< 0.001	0.12	0.73	71.16	< 0.001	26.40	< 0.001
TW C	20.40	< 0.001	33.56	< 0.001	8.18	< 0.001	6.60	0.02	69.96	< 0.001	9.31	< 0.001
Protein												
RA R	2.41	0.13	10.05	< 0.001	3.10	0.01	0.00	0.99	11.35	< 0.001	4.57	< 0.001
RA M	21.83	< 0.001	61.46	< 0.001	17.49	< 0.001	6.19	0.02	31.84	< 0.001	7.67	< 0.001
RA C	0.55	0.46	5.80	< 0.001	2.00	0.05	1.66	0.21	9.42*	< 0.001	1.43*	0.23
TW R	0.54	0.47	14.10	< 0.001	8.83	< 0.001	3.57	0.07	9.14	< 0.001	3.57	< 0.001
TW M	2.40	0.13	33.03	< 0.001	18.25	< 0.001	10.71	0.002	39.84	< 0.001	11.62	< 0.001
TW C	0.12	0.73	7.061	< 0.001	2.50	0.02	0.91	0.35	6.84†	< 0.001	2.03†	0.06

TABLE 1B. Rectangular vs. twilight light-to-dark transitions (two-way ANOVA comparing *Per1* and *Per2* mRNA and PER1 and PER2 protein levels)

	Per1						*Per2*					
	LD transition		Time		Interaction		LD transition		Time		Interaction	
	F_1-value	*P*-value	F_{12}-value	*P*-value	F_{12}-value	*P*-value	F_1-value	*P*-value	F_{12}-value	*P*-value	F_{12}-value	*P*-value
mRNA												
S R	38.08	< 0.001	47.21	< 0.001	5.49	< 0.001	37.45	< 0.001	106.7	< 0.001	6.30	< 0.001
S M	13.66	< 0.001	86.38	< 0.001	7.92	< 0.001	16.30	< 0.001	147.9	< 0.001	9.47	< 0.001
S C	18.36	< 0.001	45.40	< 0.001	4.94	< 0.001	16.27	< 0.001	88.99	< 0.001	2.77	0.005
L R	8.28	0.01	38.58	< 0.001	2.54	0.008	125.7	< 0.001	49.87	< 0.001	1.33	0.22
L M	4.45	0.04	38.58	< 0.001	1.37	0.20	89.1	< 0.001	51.39	< 0.001	1.63	0.10
L C	19.29	< 0.001	70.03	< 0.001	1.43	0.18	57.31	< 0.001	78.41	< 0.001	3.68	< 0.001
Protein												
S R	10.81	0.002	22.45	< 0.001	2.43	0.02	6.52	0.014	15.62	< 0.001	2.08	0.04
S M	3.65	0.06	95.65	< 0.001	9.26	< 0.001	0.89	0.35	55.72	< 0.001	2.18	0.03
S C	1.55	0.22	9.93	< 0.001	1.47	0.18	7.37	0.02	9.96†	< 0.001	1.86†	0.09
L R	3.17	0.08	9.82	< 0.001	1.36	0.22	19.85	< 0.001	8.70	< 0.001	0.48	0.91
L M	1.06	0.31	32.75	< 0.001	1.45	0.18	1.72	0.20	27.63	< 0.001	1.74	0.09
L C	4.13	0.05	3.55	< 0.001	0.97	0.49	5.18	0.03	5.58*	< 0.001	1.35*	0.26

TABLE 1C. Rostral vs. middle vs. caudal SCN (two-way ANOVA comparing *Per1* and *Per2* mRNA and PER1 and PER2 protein levels)

	Per1						*Per2*					
	SCN part		Time		Interaction		SCN part		Time		Interaction	
	F_1-value	*P*-value	F_{12}-value	*P*-value	F_{12}-value	*P*-value	F_1-value	*P*-value	F_{12}-value	*P*-value	F_{12}-value	*P*-value
mRNA												
S RA	14.02	< 0.001	117.72	< 0.001	2.09	< 0.001	5.97	0.004	183.30	< 0.001	2.71	< 0.001
L RA	4.31	0.02	47.16	< 0.001	9.18	< 0.001	5.38	0.006	58.90	< 0.001	5.09	< 0.001
S TW	1.95	0.15	59.42	< 0.001	0.94	0.55	0.49	0.61	146.51	< 0.001	0.98	0.51
L TW	1.74	0.18	72.76	< 0.001	5.61	< 0.001	7.96	< 0.001	120.90	< 0.001	5.93	< 0.001
Protein												
S RA	41.20	< 0.001	43.58	< 0.001	3.77	< 0.001	101.83	< 0.001	20.34	< 0.001	4.69	< 0.001
L RA	98.41	< 0.001	13.79	< 0.001	2.92	< 0.001	33.39	< 0.001	22.37*	< 0.001	6.97	< 0.001
S TW	58.18	< 0.001	52.80	< 0.001	2.86	< 0.001	32.08	< 0.001	31.71†	< 0.001	3.26	< 0.001
L TW	59.15	< 0.001	19.09	< 0.001	2.59	< 0.001	66.01	< 0.001	17.29	< 0.001	3.33	< 0.001

*F_{10}-value; †F_{11}-value (applies to Tables 1A, 1B and 1C).

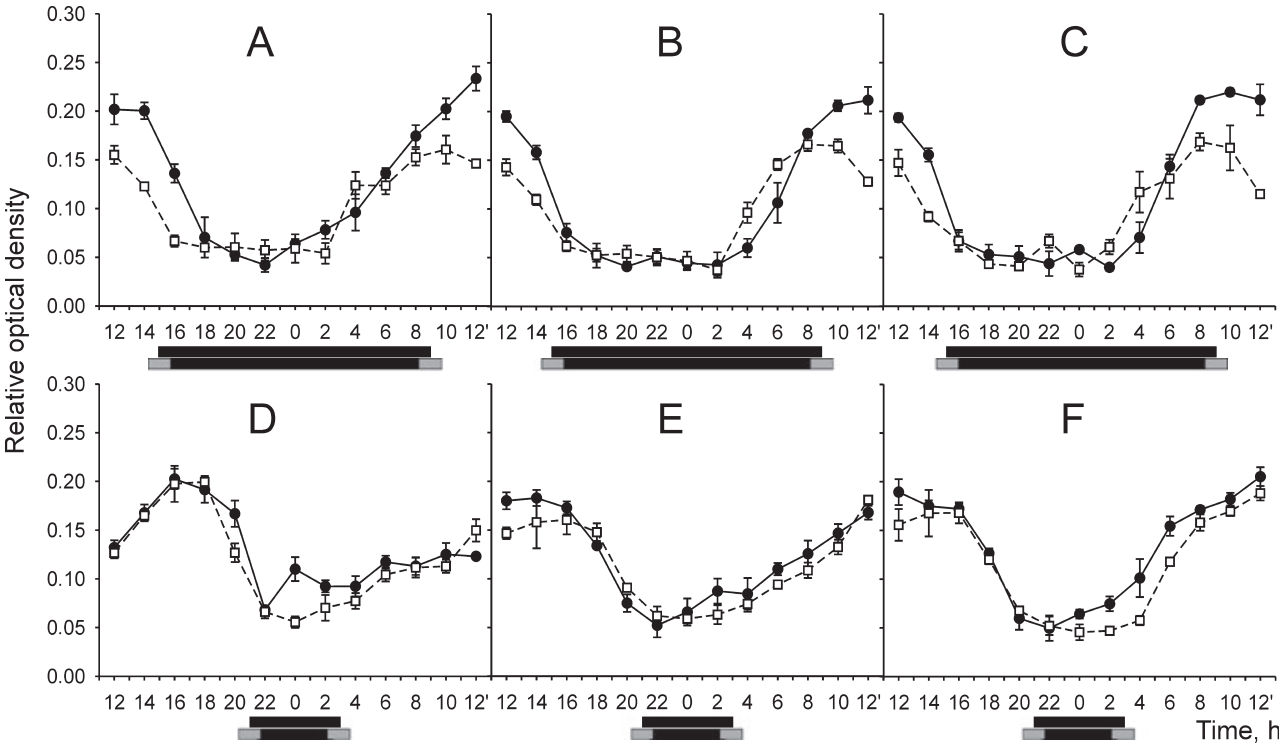

FIG. 2. Daily profiles of *Per1* mRNA levels within the rostral (A, D), middle (B, E) and caudal (C, F) part of the SCN of mice entrained to a short (A–C) or a long photoperiod (D–F) with a RA (solid line) or TW (dashed line) LD transition. Mice were released into darkness on the day of sampling. Data are expressed as relative optical density (OD). Each point represents mean ± SEM from four animals. Dark bars below the profiles depict intervals of the previous darkness; the upper bar indicates the photoperiod with RA and the lower bar with TW LD transition.

12.00 h ($P < 0.01$), between R- and M-SCN at 12.00, 18.00, 20.00, 00.00 and 12.00 h ($P < 0.01$), and between M- and C-SCN at 06.00, 08.00, 10.00 and 12.00 h ($P < 0.01$). In TW, the profiles between R- and C-SCN differed at 16.00 h ($P < 0.05$), 18.00, 20.00, 08.00, 10.00 and 12.00 h ($P < 0.01$), between R- and M-SCN at 16.00 h ($P < 0.02$), 18.00 and 20.00 h ($P < 0.01$), and between the M- and C-SCN at 18.00 h ($P < 0.05$), 08.00 and 10.00 h ($P < 0.01$). The cross-correlation analysis revealed a significant phase-delay in the profile in R- as compared with those in C- and M-SCN for RA ($R = 0.800$, $P < 0.002$ and $R = 0.723$, $P < 0.008$, respectively) as well as for TW ($R = 0.916$ and $R = 0.879$, respectively, both $P < 0.001$). No phase-shifts between the profiles in the M- and C-SCN were detected under the long RA and TW photoperiods.

Altogether, the profiles of *Per1* mRNA under the short TW photoperiod were phase-advanced relative to those under the short RA photoperiod within all parts of the SCN. Under the long photoperiod, *Per1* expression in TW declined in synchrony with that in RA within all parts of the SCN. In the R-SCN a significant rise occurred much later under RA than TW due to an extremely long interval of intermediate *Per1* mRNA levels that spanned half of the RA profile. However, an earlier rise of *Per1* expression under the long RA than TW photoperiod was detected in the M- and C-SCN. When the R-, M- and C-SCN *Per1* expression profiles were compared under the short photoperiod, the decline in the R-SCN was significantly phase-delayed as compared with that in the C- and M-SCN under RA, but all the SCN parts were in synchrony under the TW photoperiod. The better synchrony among the R-, M- and C- parts in the short photoperiod found under TW as compared with that under RA was just suggested for profiles under the long TW photoperiod: the significance of differences between the R-, M- and C-SCN profiles as well as the number of time points when the individual parts differed in *Per1* mRNA levels were lower under the long TW than RA photoperiod.

PER1 protein

The two-way ANOVA revealed that the PER1 protein profiles in the R-, M-, and C-SCN under the long photoperiod differed from those under the short photoperiod, whether under RA or TW conditions. Although the effect of photoperiod was significant only for the M-SCN under RA, significant interaction effects were found in the R- and C-SCN (Table 1). When PER1 protein profiles under the RA and TW photoperiods were compared under the short photoperiod, the two-way ANOVA revealed a significant difference between the profiles only in the R-SCN but not in the M- and C-SCN; however, a significant interaction effect was found in the M-SCN. Under the long photoperiod, the profiles differed significantly in the C-SCN only, but the interaction effect was not significant (Table 1).

A subsequent analysis revealed that under the short photoperiod, the decline in the PER1 level in the R-SCN (Fig. 4A) occurred simultaneously while under RA and TW (at 00.00 vs. 20.00 h, both $P < 0.05$). The rise, however, started earlier in TW (at 12.00 vs. 06.00 h, $P < 0.01$) than in RA (at 14.00 vs. 08.00 h, $P < 0.01$); the cross-correlation analysis revealed a significant 2-h phase-advance in PER1 rise under TW as compared with RA ($R = 0.926$, $P = 0.008$). In the M-SCN (Fig. 4B), the decline in the PER1 levels started earlier under TW (at 20.00 vs. 18.00 h, $P < 0.01$) than under RA (at 22.00 vs. 20.00 h, $P < 0.01$), but it was accomplished at about the same time under both RA and TW (at 00.00 vs. 20.00 h, $P < 0.01$ and vs. 22.00 h, $P < .01$, respectively). The rise also started earlier under TW (at 10.00 vs. 06.00 h, $P < 0.05$) than under RA (at 12.00 vs. 08.00 h,

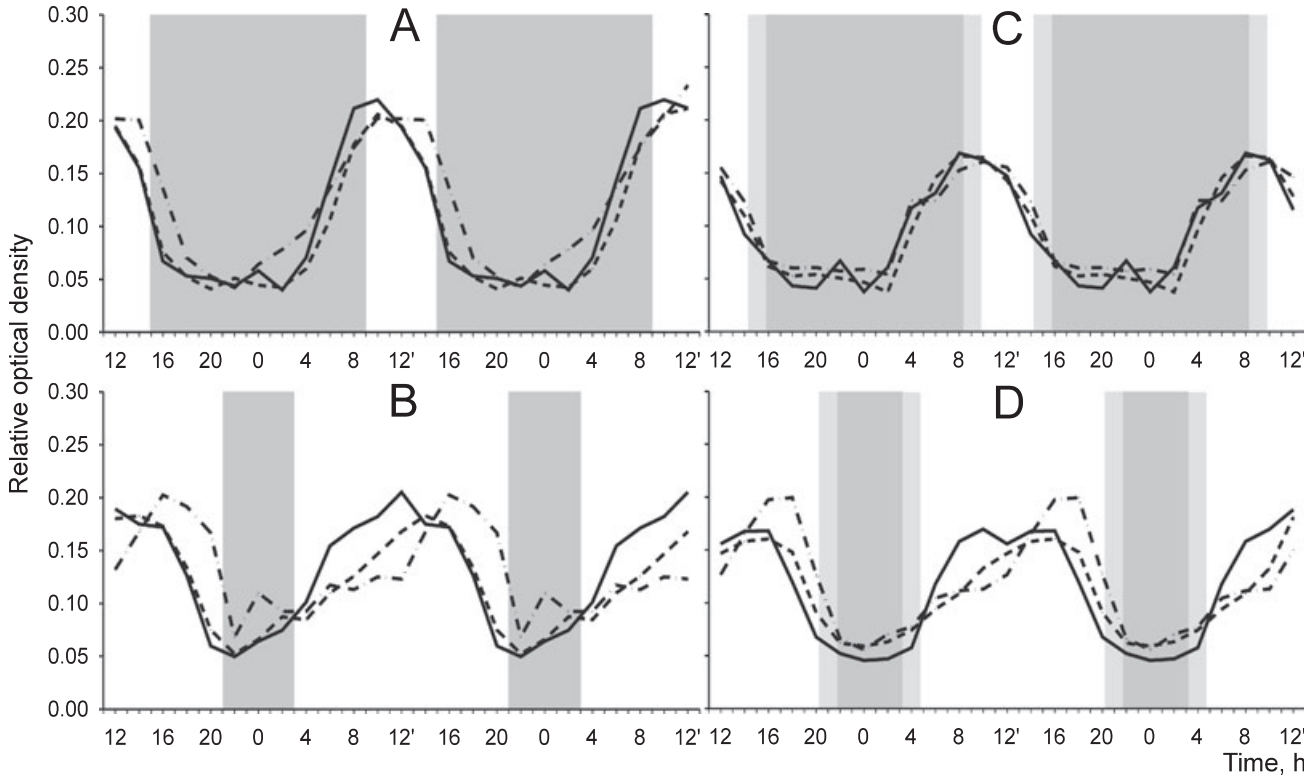

FIG. 3. Comparison of the *Per1* expression profiles within the R, M and C parts of the SCN in rats maintained under the long and short photoperiod with RA and TW LD transition. To visualize the phase relationship between the individual parts of the SCN under a particular photoperiod, the data from Fig. 2 were double-plotted, and the profiles of the R (dash dotted line), M (dashed line) and C (solid line) parts were depicted on the same graph. The gray columns represent the duration of the previous dark phase under the short (A, C) or long (B, D) photoperiods with RA (A, B) or TW (C, D) LD transition. For full data with means and SEM, see Fig. 2.

$P < 0.05$). Moreover, the cross-correlation analysis revealed a significant 2-h phase-advance in the rise in PER1 levels in the M-SCN under TW as compared with that under RA ($R = 0.971$, $P < 0.001$). In the C-SCN, though the effect of time was significant (Table 1), the subsequent analysis did not reveal any significant variations in PER1 levels between individual time points (Fig. 4C), probably due to the lower number of samples at three time points. Nevertheless, the cross-correlation analysis revealed a significant 2-h phase-advance in the PER1 rise under TW as compared with that under RA ($R = 0.967$, $P < 0.002$). Thus, under the short TW photoperiod the rise in PER1 levels in all parts of the SCN was advanced by about 2 h compared with that under the short RA photoperiod. Under the long photoperiod, the subsequent analysis did not reveal any significant variations in the C-SCN between individual time points under RA or TW (Fig. 4F; Table 1). Moreover, also the cross-correlation analysis did not reveal any significant shift between the profile under RA and that under TW photoperiod in the C-SCN. Therefore, the PER1 profiles under the long RA and TW photoperiods were in synchrony within the entire SCN.

Two-way ANOVA comparison of PER1 profiles among the R-, M- and C-SCN revealed that the profiles were significantly different (Table 1). When the R- and C-SCN were compared, the PER1 profiles differed only at few time points, namely at 20.00 h under the short TW photoperiod ($P = 0.044$), at 20.00 h ($P < 0.001$) and 04.00 h ($P = 0.018$) under the long RA, and at 22.00 h ($P = 0.007$) and 02.00 h ($P = 0.019$) under the long TW photoperiod. In contrast, the M-SCN profile was significantly different from those in the R- and C-SCN at most of the time points when PER1 levels were elevated, i.e. during the interval 16.00–20.00 h under the short RA and 10.00–22.00 h under the short TW photoperiod. Under the long RA photoperiod, levels in M-SCN were significantly elevated above those in the R-SCN during the interval 10.00–02.00 (with the exception at 14.00 h) and those in the C-SCN at all time points, with the exception at 14.00 and 12.00 h. Under the long TW photoperiod, levels in M-SCN were significantly higher than those in the R-SCN during the interval of 14.00–00.00 h and above those in the C-SCN during 14.00–04.00 h (with the exception at 16.00 h). The higher amplitude of the M-SCN rhythms reflects the fact that the area of the M-SCN where PER1-immunoreactive cells are counted is about double that of the R- or C-SCN. When phases of the R- and C-SCN profiles were compared, the cross-correlation analysis revealed a 2-h phase-advance in the PER1 profile in the C-SCN compared with R-SCN under the long RA ($R = 0.877$, $P < 0.001$) and TW ($R = 0.751$, $P = 0.005$) photoperiods, but not under the short photoperiods.

In conclusion, under the short photoperiod the PER1 rise in TW preceded that in RA within all SCN parts. The PER1 profile in the C-SCN was phase-advanced by 2 h relative to that in the R-SCN under the long, but not under the short, photoperiod with RA or TW.

Comparison of daily profiles of Per2 *mRNA and PER2 protein levels in mice entrained to the long or short photoperiod with RA and TW within the R-, M- and C- part of the SCN*

Per2 *mRNA*

In the R-, M- and C-SCN, *Per2* mRNA profiles with RA under the long photoperiod differed from those under the short photoperiod, and

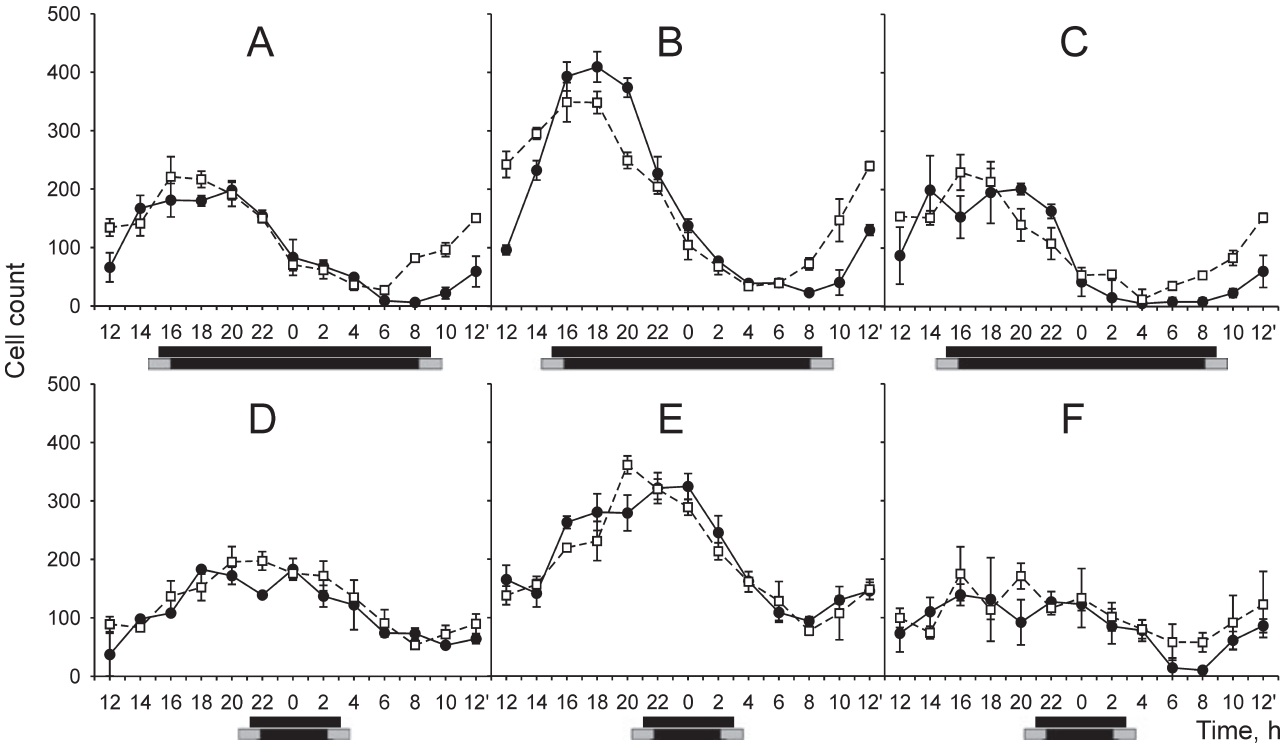

FIG. 4. Daily profiles of PER1 levels within the R (A, D), M (B, E) and C (C, F) part of the SCN of mice entrained to a short (A–C) or a long photoperiod (D–F) with a RA (solid line) or TW (dashed line) LD transition. The mice were released into darkness on the day of sampling. Data are expressed as relative OD. Each point represents mean ± SEM from three animals (only two at 12.00, 02.00 and 04.00 h). Dark bars below the profiles depict intervals of the previous darkness; the upper bar indicates the photoperiod with RA and the lower bar with TW LD transition.

in TW the difference was strongly suggested by highly significant interaction effects (Table 1). Further, these profiles were significantly modulated by the type of LD transition (Table 1).

Under the short photoperiod, the *Per2* mRNA level in the R-SCN (Fig. 5A) began to decline earlier in TW (18.00 vs. 16.00 h; $P < 0.01$) than in RA (20.00 vs. 18.00 h; $P < 0.01$), reaching its low level at 20.00 h in TW and 22.00 h in RA. The rise in *Per2* mRNA levels occurred at approximately the same time in RA and TW (08.00 vs. 06.00 h, $P < 0.01$). The cross-correlation analysis revealed a significant 2-h phase-advance in the decline of *Per2* mRNA levels in TW compared with RA ($R = 0.985$, $P < 0.001$). In the M-SCN (Fig. 5B), the decline in *Per2* mRNA levels occurred at approximately the same time in RA and TW; it started between 14.00 and 16.00 h in RA, and between 16.00 and 18.00 h in TW, and continued until 20.00 h under both conditions ($P < 0.01$). The rise occurred at 06.00 h (vs. 04.00 h, $P < 0.01$) in TW, but only at 08.00 h (vs. 06.00 h, $P < 0.01$) in RA. The cross-correlation analysis revealed a significant 2-h phase-advance in the *Per2* mRNA rise in TW as compared with RA ($R = 0.984$, $P < 0.001$). In the C-SCN (Fig. 5C), the *Per2* mRNA levels declined at 18.00 h (vs. 14.00 h, $P < 0.01$) in RA and TW, and the decline continued further until 20.00 h (vs. 18.00 h, $P < 0.01$). The significant rise occurred at 06.00 h (vs. 02.00 h, $P < 0.01$) under TW, but only at 08.00 h (vs. 06.00 h, $P < 0.01$) under RA. The cross-correlation revealed a significant 2-h phase-advance in the *Per2* mRNA rise in TW as compared with RA ($R = 0.983$, $P = 0.003$). Thus, under the short photoperiod, the *Per2* mRNA decline in the R-SCN, or rise in the M- and C-SCN in TW, appeared to be phase-advanced relative to that in RA.

Under the long photoperiod, the two-way ANOVA revealed significant differences between *Per2* mRNA profiles in RA and TW in all parts of the SCN (Table 1). However, in the R- and M-SCN, different mean values of the profiles under RA and TW resulted in non-significant interaction effects. *Per2* mRNA levels in the R-SCN (Fig. 5D) declined at the same time in RA and TW, i.e. at 00.00 h (as compared with 22.00 h, $P < 0.01$). The rise in *Per2* mRNA levels was slow and gradual under both TW and RA. It was significant at 08.00 h (vs. 06.00 h, $P < 0.01$) in TW and at 10.00 h (vs. 04.00 h, $P < 0.01$) in RA. The cross-correlation analysis revealed a significant 2-h phase-advance in the *Per2* mRNA rise in TW as compared with RA ($R = 0.985$, $P = 0.002$). Within the M-SCN (Fig. 5E), the *Per2* mRNA declined in RA and TW simultaneously, i.e. at 00.00 h (vs. 22.00 h, $P < 0.01$). A significant rise occurred at 06.00 and 08.00 h (as compared with 04.00 h, both $P < 0.01$) in RA and TW, respectively. The cross-correlation revealed a significant 2-h phase-advance in the *Per2* mRNA rise in RA as compared with TW ($R = 0.923$, $P = 0.025$). In the C-SCN (Fig. 4F), the decline in the *Per2* mRNA level occurred at about the same time in RA and TW, i.e. at 22.00 h (vs. 20.00 h in RA, $P < 0.01$; and vs. 14.00 h in TW, $P < 0.05$), though the decline was more gradual in TW than in RA. The rise also occurred simultaneously in RA and TW, and was significant for the first time at 08.00 h (vs. 06.00 h, $P < 0.01$).

Comparison of *Per2* mRNA profiles among the R-, M- and C-SCN under the short photoperiod (Fig. 7A and C) revealed that there was a significant difference between the individual parts of the SCN in RA, but not in TW (Table 1). The *post hoc* analysis revealed that under the short RA photoperiod, the *Per2* mRNA levels at 04.00 h were significantly higher in the C-SCN than in the M-SCN ($P < 0.05$), at 08.00 h they were higher in the C- and M-SCN than in the R-SCN ($P < 0.05$ and $P < 0.01$, respectively), at 16.00, 18.00 and 20.00 h

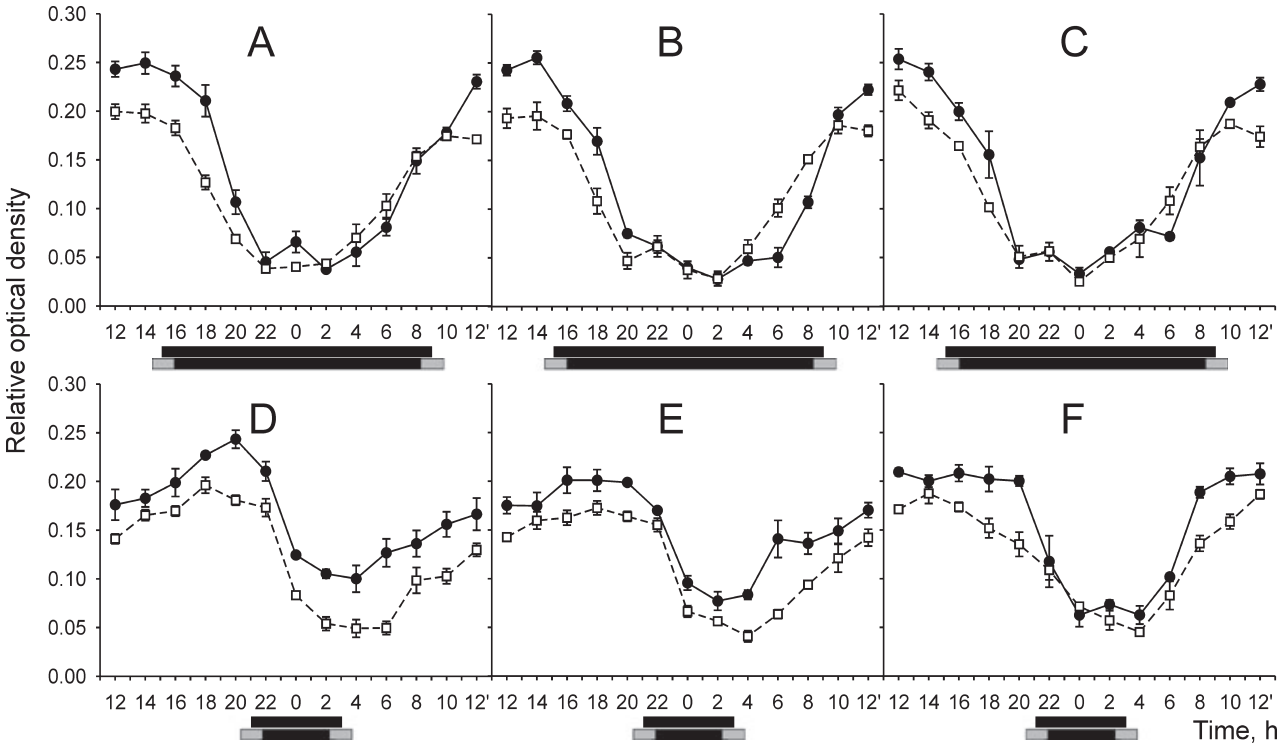

FIG. 5. Daily profiles of *Per2* mRNA levels within the R (A, D), M (B, E) and C (C, F) part of the SCN of mice entrained to a short (A–C) or a long photoperiod (D–F) with RA (solid line) or TW (dashed line) LD transition. For other details, see legend to Fig. 2.

they were higher in the R- than in the C-SCN ($P < 0.05$, $P < 0.01$ and $P < 0.01$, respectively), and at 18.00 and 20.00 h they were higher in the R- than in the M-SCN ($P < 0.01$). The cross-correlation analysis did not reveal any significant phase-shift among the *Per2* profiles in the R-, M- and C-SCN under the short RA. However, when a phase-shift in the decline was tested separately, the cross-correlation analysis revealed a 2-h phase-delay of the decline in the R-SCN as compared with the C-SCN ($R = 0.970$, $P < 0.001$). Under the long photoperiod (Fig. 6B and D), there was a significant difference between the individual parts of the SCN in RA and TW (Table 1). Under the long RA photoperiod, the *Per2* mRNA levels differed significantly between R- and C-SCN at 20.00, 22.00, 00.00, 08.00 and 10.00 h ($P < 0.01$), and at 04.00 and 12.00 h ($P < 0.05$), between R- and M-SCN at 20.00 h ($P < 0.01$) and 22.00 h ($P < 0.05$), and between M- and C-SCN at 22.00, 08.00, 10.00 ($P < 0.01$) and at 00.00, 06.00 and 12.00 h ($P < 0.05$). In TW, the levels between R- and C-SCN differed at 18.00, 20.00, 22.00, 06.00, 08.00, 10.00 and 12.00 h ($P < 0.01$) and at 12.00 h ($P < 0.05$), between R- and M-SCN only at 18.00 h ($P < 0.05$), and between M-and C-SCN at 12.00, 08.00, 10.00, 12.00 h ($P < 0.01$) and at 20.00 h ($P < 0.05$). The cross-correlation analysis demonstrated a significant phase-advance in the *Per2* expression profile in the C-SCN relative to that in the R-SCN in RA ($R = 0.863$, $P < 0.001$), as well as in TW ($R = 0.869$, $P < 0.001$).

Altogether, under the short photoperiod, the profiles of *Per2* mRNA in TW seemed to be phase-advanced, relative to those in RA, within all parts of the SCN. Under the long photoperiod, the *Per2* mRNA rise under TW occurred earlier than under RA in the R-SCN, later in the M-SCN and at the same time in the C-SCN; the decline was simultaneous in all the SCN parts. Hence under the long photoperiod, only the rise of *Per2* expression in the R-SCN was significantly affected by the type of LD transition. Under the short RA photoperiod the *Per2* mRNA decline in the R-SCN was significantly phase-delayed compared with that in the C-SCN, while under the short TW photoperiod all parts of the SCN were in synchrony. Under the long RA and TW photoperiods, the R-SCN profile was significantly delayed, relative to the C-SCN profile. However, under the long TW photoperiod, a higher degree of synchrony between the R-, M- and C-parts found under the short TW photoperiod was still suggested as compared with the long RA photoperiod, namely due to the synchrony between the profiles in the R- and M-SCN.

PER2 protein

The two-way ANOVA revealed that PER2 protein profiles were different under the long and short photoperiod in the R- and M-, but not within the C-SCN, whether under RA or TW (Table 1). When PER2 protein profiles under RA were compared with those under TW (Table 1), the two-way ANOVA revealed significant differences between the profiles in the R- and C-SCN both under the long and short photoperiod, but the interaction effect was significant only in the R-SCN under the short photoperiod. In the M-SCN, the difference between RA and TW was not significant under the short and long photoperiod, but under the short photoperiod there was a significant interaction effect (Table 1). Under the short photoperiod, the PER2 decline in RA in the R-SCN (Fig. 7A) was significant for the first time at 22.00 h (vs. 20.00 h, $P < 0.05$) and in TW at 02.00 h (vs. 20.00 h, $P < 0.05$), but the minimum levels were achieved at 02.00 h, i.e. at about the same time under both LD transitions. PER2 levels began to gradually rise earlier in TW than RA, but significantly elevated levels were achieved at the same time, i.e. at 18.00 vs. 12.00 h ($P < 0.01$) in RA and vs. 06.00 h ($P < 0.01$) in TW. In the M-SCN, PER2 levels declined simultaneously in RA and TW (Fig. 7B), i.e. at 22.00 h (vs. 20.00 h, $P < 0.01$), and the decline continued until 02.00 h (vs. 22.00 h, $P < 0.01$). Under RA, the first rise occurred at 14.00 h (vs. 12.00 h, $P < 0.01$) and continued until 18.00 h (vs. 14.00 h,

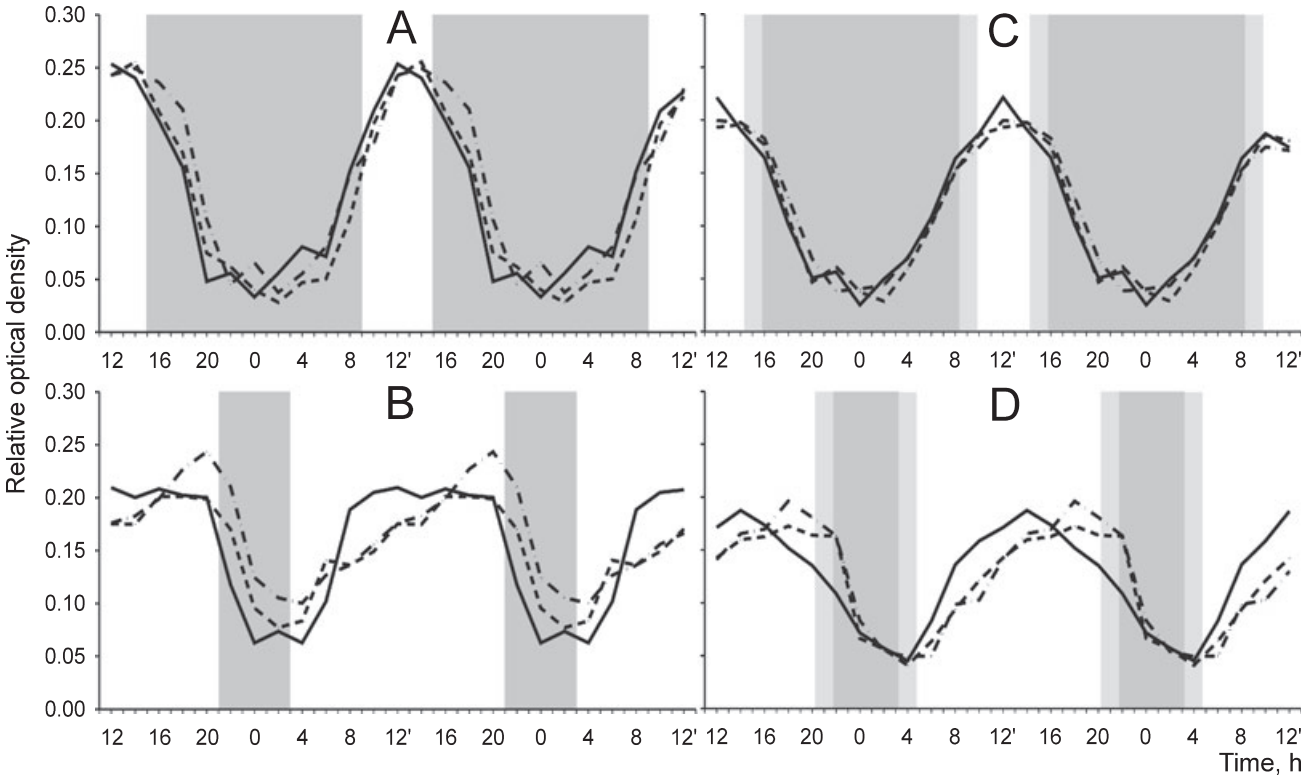

FIG. 6. Comparison of the *Per2* expression profiles in the R, M and C parts of the SCN of mice maintained under the long and short photoperiod with RA and TW LD transition. To visualize the phase relationship between the individual parts of the SCN under particular photoperiod, the data from Fig. 5 were double-plotted, and the profiles of the R (dash dotted line), M (dashed line) and C (solid line) parts were depicted in the same graph. The gray columns represent duration of the previous dark phase under the short (A, C) or long (B, D) photoperiods with RA (A, B) or TW (C, D) LD transition. For full data with means and SEM, see Fig. 5.

$P < 0.01$), whereas under TW the rise started at 12.00 h (vs. 10.00 h, $P < 0.05$) and continued until 16.00 h (vs. 14.00 h, $P < 0.01$). The cross-correlation analysis revealed a significant 2-h phase-advance in the PER2 rise in TW compared with short RA photoperiod ($R = 0.966$, $P < 0.002$). In the C-SCN (Fig. 7C), the decline in RA and TW appeared to be simultaneous, reaching its nadir level at 00.00 h (vs. 18.00 h in RA, $P < 0.05$, and 16.00 h in TW, $P < 0.05$). The rise was significant at 18.00 h (vs. 12.00 h, $P < 0.05$) in RA and at 16.00 h (vs. 10.00 h, $P < 0.05$) in TW. The cross-correlation analysis revealed a significant 2-h phase-advance in the PER2 rise in TW as compared with RA ($R = 0.925$, $P < 0.024$). Thus, under the short photoperiod the rise in PER2 levels in the M- and C-SCN parts under TW was advanced, compared with that under RA. Under the long photoperiod, PER2 levels within the R-SCN (Fig. 7D) decreased at 06.00 h (vs. 02.00 h, $P < 0.05$) under RA and at 08.00 h (vs. 22.00 h, $P < 0.05$) under TW. The levels increased significantly at 18.00 h (vs. 06.00 h, $P < 0.05$) in RA and at 22.00 h (vs. 12.00 h, $P < 0.05$) in TW. However, the cross-correlation analysis did not reveal any significant phase-shift between the RA and TW profiles. In the M-SCN (Fig. 7E), no significant difference between the profile under the long RA and that under the long TW photoperiod was revealed (Table 1) and, therefore, no *post hoc* comparisons were performed. In the C-SCN (Fig. 7F), neither the decline nor the rise in the PER2 protein under RA and TW was significant, and the cross-correlation analysis did not reveal any significant phase-shift between the RA and TW photoperiods. Therefore, under the long photoperiod, PER2 profiles in RA were in synchrony with those in TW in all SCN parts.

The two-way ANOVA revealed significant differences among PER2 profiles in the R-, M- and C-SCN (Table 1). Similar to PER1, the PER2 profiles in the R- and C-SCN differed only at a few time points, namely under the short RA photoperiod at 18.00 h ($P = 0.035$), 20.00 h ($P < 0.001$) and 00.00 h ($P = 0.038$), under the short TW photoperiod at 22.00 h ($P = 0.031$), and under the long TW photoperiod at 22.00 h ($P < 0.001$) and 00.00 h ($P = 0.020$). Under the long RA photoperiod, no difference between the R- and C-SCN was found. The M-SCN levels were significantly elevated above those in the R-SCN under the short RA photoperiod during the 12.00–04.00 h interval (with the exception of values at 14.00 and 18.00 h), under the short TW photoperiod at 12.00 h and between 16.00 and 20.00 h, under the long RA photoperiod during the 16.00–20.00 h interval, and under the long TW photoperiod between 14.00 and 00.00 h. Similarly, the M-SCN levels were significantly higher than those in the C-SCN under the short RA photoperiod between 12.00 and 02.00 h (with the exception of the value at 14.00 h), under the short TW photoperiod at 12.00 h and between 16.00 and 22.00 h, under the long RA photoperiod between 16.00 and 22.00 h, and under the long TW photoperiod between 14.00 and 02.00 h. Similar to PER1 profiles, the higher PER2 amplitude of the M-SCN rhythms reflects larger area of the M-SCN where PER2-immunopositive cells were counted as compared with the R- and C-SCN. When phases of the R- and C-SCN profiles were compared, the cross-correlation analysis revealed a 2-h phase-advance in the PER2 profile in the C-SCN, compared with that in the R-SCN under the long RA ($R = 0.857$, $P = 0.002$) and TW ($R = 0.676$, $P = 0.016$) photoperiods, but not under the short photoperiods.

In conclusion, under the short photoperiod the PER2 rise in TW was phase-advanced significantly relative to that in RA in the M- and C-SCN. Under the long photoperiod, the PER2 profile in RA was in synchrony with that in TW in all parts of the SCN. The PER2 profile

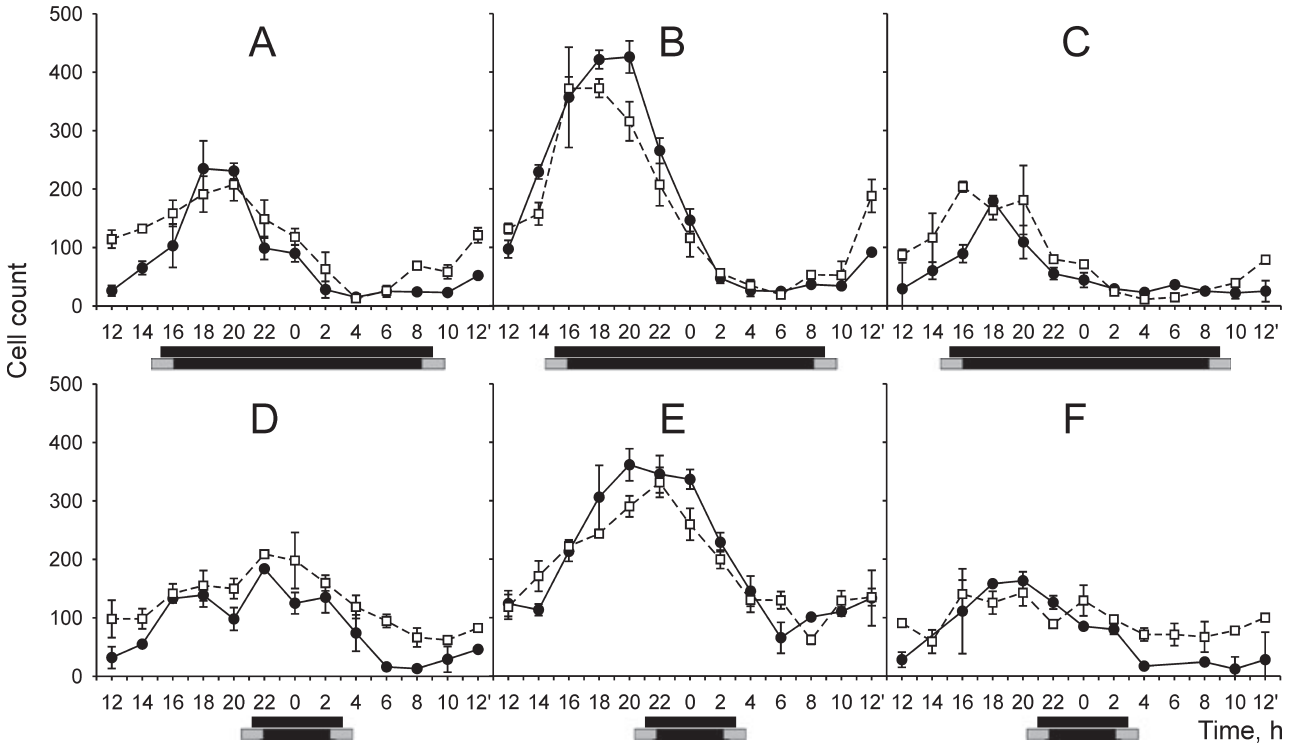

FIG. 7. Daily profiles of PER2 levels within the R (A, D), M (B, E) and C (C, F) part of the SCN of mice entrained to a short (A–C) or a long photoperiod (D–F) with RA (solid line) or TW (dashed line) LD transition. For other details, see legend to Fig. 4.

in the C-SCN was phase-advanced by 2 h relative to the profile in the R-SCN under the long RA and TW photoperiods, but not under the short RA and TW photoperiods.

Discussion

Our data demonstrate that the type of LD transition at dawn and dusk, i.e. RA or TW, affects photoperiodic modulation of the *Per1* and *Per2* expression and PER1 and PER2 protein profiles differently within separate parts of the mouse SCN.

Across the entire SCN, time of the evening decline and morning rise in *Per1* and *Per2* expression was affected by the photoperiod so that the duration of high *Per1* and *Per2* mRNA levels was shorter under the short photoperiod with only 6 h of daylight than under the long photoperiod with 18 h of daylight, whether under RA or TW conditions. This finding was in accordance with numerous previously published data (for review, see Daan *et al.*, 2001; Sumová *et al.*, 2004). When separate parts of the SCN were compared under the short and long photoperiod, the difference in duration of the interval between the rise and decline of *Per1* and *Per2* expression levels appeared to be present only in the C- and M-, but not in the R-SCN under the photoperiod with RA or TW. Thus, duration of high *Per1* and *Per2* expression was longer under the long than under the short photoperiod only in the M- and C-SCN parts, similar to previous studies when representative sections from the mid-caudal position in the rat SCN were studied (Sumová *et al.*, 2003, 2007). The PER1 protein profile in the M-SCN was also modulated by the photoperiod, similar to that seen in rats (Sumová *et al.*, 2002). Moreover, the present study in mice indicated photoperiodic modulation also of the PER2 protein profile within the M-SCN.

In addition, the data showed that phases of *Per1* and *Per2* expression profiles in the R-, M- and C-SCN were more synchronized with each other under the short than under the long photoperiods. When RA and TW LD regimes were compared, *Per1* and *Per2* profiles in the R-, M- and C-SCN were completely synchronous under the short photoperiod with TW, while in RA a 2-h delay in the *Per1* and *Per2* mRNA decline in the R-SCN, compared with other SCN parts, was detected. Under the long photoperiod, the expression profiles within the R-, M- and C-SCN parts differed significantly in RA as well as in TW. *Per1* mRNA profile in the C- and M-SCN was phase-advanced compared with that in the R-SCN both in RA and TW. Similarly, the *Per2* mRNA profile in the C-SCN was advanced to that in the R-SCN, again both in RA and TW. However, better synchronization among the individual parts in TW than in RA was indicated, similar to the situation under the short photoperiod, due namely to a lower number of time points when mRNA levels differed significantly among the individual SCN parts. At the protein level, PER1 and PER2 profiles were synchronized among the R-, M- and C-SCN under the short RA and TW photoperiods. Under the long RA and TW photoperiods, the C-SCN profiles phase-led by 2 h those in the R-SCN. Similarly to the mRNA profiles, differences between the R- and C-SCN protein profiles were more pronounced in the RA than in the TW photoperiod, due namely to higher statistical significance. The effect of the TW condition on synchrony among the individual SCN parts was thus significant under the short photoperiod and suggested under the long one.

Previous studies on the inter-phasing of the SCN cell subpopulations explored RA photoperiods only. In Siberian hamsters, exposure to a long photoperiod with 16 h of daylight induced desynchrony among *Per2*, *Rev-erbα* and *Dbp* expression rhythms the R- and those in the C-SCN, but not the *Avp* expression rhythms (Hazlerigg *et al.*, 2005; Johnston *et al.*, 2005). In Syrian hamsters, exposure to the same long photoperiod caused phase dispersion of the rhythms in c-FOS- and PER1-immunoreactivity, and the profiles in the C-SCN phase-led

those in the M- and R-SCN (Yan & Silver, 2008). In mice entrained to a long photoperiod with 16 h of daylight, not only *Per1* but also *Bmal1* expression profiles were advanced in the C-SCN, compared with the R-SCN (Naito *et al.*, 2008). In all of the above-mentioned studies, the rhythms in the C-SCN preceded those in the R-SCN under the long photoperiod. These data suggest that desynchrony and separation of phases in clock gene expression rhythms among individual parts of the SCN might account for the photoperiodic modulation of SCN function. In order to be 'active' for an extended time under the long photoperiod, the SCN successively 'switches on' its separate parts, the caudal part being first and the rostral part last. Consequently, under the very long photoperiod, the entire SCN may find itself in a daytime state for a much longer time than its individual parts.

Our findings on the impact of a long photoperiod on *Per1* and *Per2* expression profiles are supported by recent *in vitro* data on real-time expression recordings in SCN slices from mice entrained either to a long photoperiod with 18 h of daylight or to a short photoperiod with only 6 h of daylight. Robust circadian rhythms of *Per1-luc* activity were recorded in anterior and posterior SCN slices, with the exception for the anterior SCN slices from mice entrained to the long photoperiod. In these anterior slices, a bimodal pattern of *Per1-luc* activity was detected and the rhythm differed from that of the posterior part (Inagaki *et al.*, 2007). Concerning the protein data, no differences between the anterior and posterior SCN of mice entrained to a long photoperiod with 16 h of daylight were detected for PER2::luc activity *in vitro* (Mickman *et al.*, 2008), while in our *in vivo* study with 18 h of daylight, a 2-h phase-advance in the C-SCN PER2 profile was revealed compared with the R-SCN profile. For the mRNA profiles, similar to our study, higher variability in gene expression within the anterior part of the SCN under the long than under the short photoperiod was reported (Inagaki *et al.*, 2007; Mickman *et al.*, 2008). According to the current hypothesis, the photoperiod affects intercellular synchrony among individual cell oscillators in the SCN (Schaap *et al.*, 2003; Rohling *et al.*, 2006; VanderLeest *et al.*, 2007). Therefore, it seems plausible to speculate that the extremely long photoperiod with 18 h of daylight and an abrupt LD transition may cause desynchrony among individual cells in the R-SCN at dawn. Such desynchrony might be reflected by a long interval of intermediate levels of *Per1* mRNA sustaining across half of the daily expression profile (from CT0 to CT12) as observed in our study under the long RA photoperiod. Consequently, rhythms of the C-SCN might desynchronize from those of the R- and M-SCN. However, under the long TW photoperiod, the expression profiles within the R- and M-SCN were in synchrony with each other. Therefore, we can speculate that TW might attenuate the effect of a long photoperiod on synchrony among the SCN regions.

The data further demonstrate that under the short photoperiod, *Per1* and *Per2* mRNA profiles, as well as PER1 and PER2 rise, in TW were phase-advanced relative to those in RA. The *Per1* and *Per2* expression profiles in R-, M- and C-SCN were affected differently. The evening decline in *Per1* and *Per2* expression, but not the morning rise, was advanced in the R-SCN, while in the M- and C-SCN, mostly the morning rise was advanced. For the protein profiles, only the rise in PER1 and PER2 levels, but not the decline, was phase-advanced in all SCN parts, with the exception of PER2 in the R-SCN. The possibility that slight differences in the duration of the almost complete darkness between the RA and TW regimes might account for the phase differences cannot be ruled out. In our experimental arrangement, the light intensity under the TW conditions decreased gradually, and at the time of lights-off in RA there was still 1 lx in the TW photoperiod. The light intensity declined further, so that after 22 min there was 0.1 lx and after 45 min it reached 0.01 lx. Similarly, lights-on in the TW condition started from the level of 0.01 lx 45 min before the lights-on in RA, increased to 0.1 lx 22 min later and reached 1 lx at the time of the lights-on in RA. Nevertheless, the overall observed earlier phase of the profiles of *Per* gene expression and protein levels under TW than under RA short photoperiods is in agreement with previously published data on the locomotor activity rhythm in hamsters (Boulos *et al.*, 1996a, 2002; Boulos & Macchi, 2005). In these studies, timing of the locomotor activity onset and offset also occurred earlier in the short photoperiods with TW than with RA. Moreover, the presence of TW resulted in a lower variability in the locomotor activity rhythm. Based on these data, a hypothesis was formulated that LD transitions with TW might increase the strength of the LD cycle as an entraining cue.

Last, but not least, also under the long photoperiod the expression profiles of both *Per* genes were entrained with a slight difference depending on whether the LD transition was abrupt or gradual. Under the long TW photoperiod, the *Per1* and *Per2* mRNA rise was advanced, relative to that under RA in the R-SCN only, but delayed or not affected by the LD transition in other parts of the SCN. The data suggest that the extremely long 18-h photoperiod with an abrupt LD transition might cause desynchrony among cells in the R-SCN responding to dawn but not between those responding to dusk. Consequently, the significant rise in *Per1* expression in the whole population of the R-SCN cells in RA was postponed as compared with that in TW. If this were the case, TW might be more able to maintain synchrony among the SCN cells, compared with RA and, therefore, the rise in *Per1* and *Per2* expression in the population of the R-SCN cells may be achieved earlier. In contrast to the short photoperiod, no differences in PER1 and PER2 profiles between the long RA and the long TW photoperiod were detected in any part of the SCN.

Importantly, all the findings were obviously not due to a masking effect of the RA or TW transitions, because all profiles were examined after releasing mice into constant darkness. We are, however, aware of the fact that the TW simulation used did not have some aspects of the natural twilight. Although changes in spectral composition during the natural twilight periods are small (Hut *et al.*, 2000), they may play a role in circadian entrainment and photoperiodic responses. It is also important to note that the maximal light intensity of 100 lx used in this study might be three orders of magnitude lower than light intensities reached in nature. Therefore, more pronounced differences might be likely found if natural photoperiods with twilight were used. Also, while nocturnal animals living under natural conditions often only 'sample' light for a few minutes a day, spending most of the time underground (DeCoursey, 1986), our mice were maintained under LD conditions in standard cages without a den.

In conclusion, our results suggest that a TW photoperiod provides better synchrony among populations of the SCN molecular oscillators than a RA one. The effect of twilight is stronger under conditions when organisms are exposed to extremely short photoperiods, compared with long ones.

Acknowledgements

The authors gratefully acknowledge Professor Hitoshi Okamura (Kobe University School of Medicine, Japan) for Per1 and Per2 cDNA fragments used in the *in situ* hybridization, Professor Helena Illnerová for her helpful comments on the manuscript, Alena Dědičová for her help with statistical analysis, and Eva Suchanová for her excellent technical assistance. The study was supported by the 6th Framework Project EUCLOCK 018741, grant 309080503, and by Research Projects AV0Z 50110509 and LC554.

Abbreviations

C-SCN, caudal part of the suprachiasmatic nucleus; LD, light–dark regimen; LD18 : 6, light–dark regimen with 18 h of light and 6 h of darkness; LD6 : 18, light–dark regimen with 6 h of light and 18 h of darkness; M-SCN, middle part of the suprachiasmatic nucleus; OD, optical density; PBS, phosphate-buffered saline; RA, rectangular light-to-dark transition; R-SCN, rostral part of the suprachiasmatic nucleus; SCN, suprachiasmatic nuclei of the hypothalamus; TW, twilight light-to-dark transition.

References

Boulos, Z. & Macchi, M.M. (2005) Season- and latitude-dependent effects of simulated twilights on circadian entrainment. *J. Biol. Rhythms*, **20**, 132–144.

Boulos, Z., Macchi, M., Houpt, T.A. & Terman, M. (1996a) Photic entrainment in hamsters: effects of simulated twilights and nest box availability. *J. Biol. Rhythms*, **11**, 216–233.

Boulos, Z., Macchi, M. & Terman, M. (1996b) Twilight transitions promote circadian entrainment to lengthening light–dark cycles. *Am. J. Physiol. Regul. Integr. Comp. Physiol.*, **271**, R813–R818.

Boulos, Z., Macchi, M.M. & Terman, M. (2002) Twilights widen the range of photic entrainment in hamsters. *J. Biol. Rhythms*, **17**, 353–363.

Daan, S. & Aschoff, J. (1975) Circadian rhythms of locomotor activity in captive birds and mammals: their variations with season and latitude. *Oecologia*, **18**, 269–316.

Daan, S., Albrecht, U., van der Horst, G.T., Illnerova, H., Roenneberg, T., Wehr, T.A. & Schwartz, W.J. (2001) Assembling a clock for all seasons: are there M and E oscillators in the genes? *J. Biol. Rhythms*, **16**, 105–116.

DeCoursey, P.J. (1986) Light-sampling behavior in photoentrainment of a rodent circadian rhythm. *J. Comp. Physiol. [A]*, **159**, 161–169.

Elliott, J.A. & Tamarkin, L. (1994) Complex circadian regulation of pineal melatonin and wheel-running in Syrian hamsters. *J. Comp. Physiol. [A]*, **174**, 469–484.

Hastings, M.H. (2001) Modeling the Molecular Calendar. *J. Biol. Rhythms*, **16**, 117–123.

Hastings, M.H., Field, M.D., Maywood, E.S., Weaver, D.R. & Reppert, S.M. (1999) Differential regulation of mPER1 and mTIM proteins in the mouse suprachiasmatic nuclei: new insights into a core clock mechanism. *J. Neurosci.*, **19**, RC11.

Hazlerigg, D.G., Ebling, F.J. & Johnston, J.D. (2005) Photoperiod differentially regulates gene expression rhythms in the rostral and caudal SCN. *Curr. Biol.*, **15**, R449–R450.

Hut, R.A., Scheper, A. & Daan, S. (2000) Can the circadian system of a diurnal and a nocturnal rodent entrain to ultraviolet light? *J. Comp. Physiol. [A]*, **186**, 707–715.

Illnerová, H. (1988) Entrainment of mammalian circadian rhythms in melatonin production by light. *Pineal Res. Rev.*, **6**, 173–217.

Illnerová, H. & Vaněček, J. (1980) Pineal rhythm in N-acetyltransferase activity in rats under different artificial photoperiods and in natural daylight in the course of a year. *Neuroendocrinology*, **31**, 321–326.

Inagaki, N., Honma, S., Ono, D., Tanahashi, Y. & Honma, K. (2007) Separate oscillating cell groups in mouse suprachiasmatic nucleus couple photoperiodically to the onset and end of daily activity. *Proc. Natl. Acad. Sci. USA*, **104**, 7664–7669.

Johnston, J.D., Ebling, F.J. & Hazlerigg, D.G. (2005) Photoperiod regulates multiple gene expression in the suprachiasmatic nuclei and pars tuberalis of the Siberian hamster (Phodopus sungorus). *Eur. J. Neurosci.*, **21**, 2967–2974.

Klein, D.C. & Moore, R.Y. (1979) Pineal N-acetyltransferase and hydroxyindole-O-methyltransferase: control by the retinohypothalamic tract and the suprachiasmatic nucleus. *Brain Res.*, **174**, 245–262.

Kováčiková, Z., Sládek, M., Bendová, Z., Illnerová, H. & Sumová, A. (2006) Expression of clock and clock-driven genes in the rat suprachiasmatic nucleus during late fetal and early postnatal development. *J. Biol. Rhythms*, **21**, 140–148.

LeSauter, J., Lehman, M.N. & Silver, R. (1996) Restoration of circadian rhythmicity by transplants of the SCN "micropunches". *J. Biol. Rhythms*, **11**, 163–171.

McFarland, W.N. & Munz, F.W. (1975) Part II: The photic environment of clear tropical seas during the day. *Vision Res.*, **15**, 1063–1070.

Meijer, J.H., Groos, G.A. & Rusak, B. (1986) Luminance coding in a circadian pacemaker: the suprachiasmatic nucleus of the rat and the hamster. *Brain Res.*, **382**, 109–118.

Mickman, C.T., Stubblefield, J., Harrington, M. & Nelson, D.E. (2008) Photoperiod alters the phase difference between activity onset in vivo and mPer2:luc peak in vitro. *Am. J. Physiol. Regul. Integr. Comp. Physiol.*, **295**, R1688–R1694.

Naito, E., Watanabe, T., Tei, H., Yoshimura, T. & Ebihara, S. (2008) Reorganization of the suprachiasmatic nucleus coding for day length. *J. Biol. Rhythms*, **23**, 140–149.

Pittendrigh, C.L. (1981) Circadian systems: entrainment. In Aschoff, J. (ed), *Biological Rhythms. Handbook of Behavioral Neurology.* Plenum, New York, pp. 95–124.

Rohling, J., Wolters, L. & Meijer, J.H. (2006) Simulation of day-length encoding in the SCN: from single-cell to tissue-level organization. *J. Biol. Rhythms*, **21**, 301–313.

Schaap, J., Albus, H., VanderLeest, H.T., Eilers, P.H., Detari, L. & Meijer, J.H. (2003) Heterogeneity of rhythmic suprachiasmatic nucleus neurons: implications for circadian waveform and photoperiodic encoding. *Proc. Natl. Acad. Sci. USA*, **100**, 15994–15999.

Shearman, L.P., Sriram, S., Weaver, D.R., Maywood, E.S., Chaves, I., Zheng, B., Kume, K., Lee, C.C., van der Horst, G.T., Hastings, M.H. & Reppert, S.M. (2000) Interacting molecular loops in the mammalian circadian clock. *Science*, **288**, 1013–1019.

Sládek, M., Sumová, A., Kováčiková, Z., Bendová, Z., Laurinová, K. & Illnerová, H. (2004) Insight into molecular core clock mechanism of embryonic and early postnatal rat suprachiasmatic nucleus. *Proc. Natl. Acad. Sci. USA*, **101**, 6231–6236.

Spoelstra, K. & Daan, S. (2008) Effects of constant light on circadian rhythmicity in mice lacking functional cry genes: dissimilar from per mutants. *J. Comp. Physiol. [A] Neuroethol. Sens. Neural. Behav. Physiol.*, **194**, 235–242.

Steinlechner, S., Jacobmeier, B., Scherbarth, F., Dernbach, H., Kruse, F. & Albrecht, U. (2002) Robust circadian rhythmicity of Per1 and Per2 mutant mice in constant light, and dynamics of Per1 and Per2 gene expression under long and short photoperiods. *J. Biol. Rhythms*, **17**, 202–209.

Sumová, A., Trávníčková, Z., Peters, R., Schwartz, W.J. & Illnerová, H. (1995) The rat suprachiasmatic nucleus is a clock for all seasons. *Proc. Natl. Acad. Sci. USA*, **92**, 7754–7758.

Sumová, A., Sládek, M., Jáč, M. & Illnerová, H. (2002) The circadian rhythm of Per1 gene product in the rat suprachiasmatic nucleus and its modulation by seasonal changes in daylength. *Brain Res.*, **947**, 260–270.

Sumová, A., Jáč, M., Sládek, M., Šauman, I. & Illnerová, H. (2003) Clock gene daily profiles and their phase relationship in the rat suprachiasmatic nucleus are affected by photoperiod. *J. Biol. Rhythms*, **18**, 134–144.

Sumová, A., Bendová, Z., Sládek, M., Kováčiková, Z. & Illnerová, H. (2004) Seasonal molecular timekeeping within the rat circadian clock. *Physiol. Res.*, **53**(Suppl 1), S167–S176.

Sumová, A., Kováčiková, Z. & Illnerová, H. (2007) Dynamics of the adjustment of clock gene expression in the rat suprachiasmatic nucleus to an asymmetrical change from a long to a short photoperiod. *J. Biol. Rhythms*, **22**, 259–267.

Sun, Z.S., Albrecht, U., Zhuchenko, O., Bailey, J., Eichele, G. & Lee, C.C. (1997) RIGUI, a putative mammalian ortholog of the Drosophila period gene. *Cell*, **90**, 1003–1011.

Takahashi, J.S., Hong, H.K., Ko, C.H. & McDearmon, E.L. (2008) The genetics of mammalian circadian order and disorder: implications for physiology and disease. *Nat. Rev. Genet.*, **9**, 764–775.

Usui, S. (2000) Gradual changes in environmental light intensity and entrainment of circadian rhythms. *Brain Dev.*, **22**(Suppl 1), S61–S64.

VanderLeest, H.T., Houben, T., Michel, S., Deboer, T., Albus, H., Vansteensel, M.J., Block, G.D. & Meijer, J.H. (2007) Seasonal encoding by the circadian pacemaker of the SCN. *Curr. Biol.*, **17**, 468–473.

Yan, L. & Silver, R. (2008) Day-length encoding through tonic photic effects in the retinorecipient SCN region. *Eur. J. Neurosci.*, **28**, 2108–2115.